Environment Protection Engineering

Vol. 39 2013 No. 1

DOI: 10.5277/EPE130103

MOHAMMAD A. BEHNAJADY[1], MALIHEH ELHAMI ALAMDARI[1], NASSER MODIRSHAHLA[1]

INVESTIGATION OF THE EFFECT OF HEAT TREATMENT PROCESS ON CHARACTERISTICS AND PHOTOCATALYTIC ACTIVITY OF TiO_2-UV100 NANOPARTICLES

The effect of heat treatment process on crystallite size, phase content, surface area, band gap energy and photocatalytic activity of TiO_2-UV100 nanoparticles were investigated. Heat treated TiO_2 nanoparticles were characterized by X-ray diffraction (XRD), Brunauer–Emmett–Teller (BET) isotherm and diffuse reflectance spectroscopy (DRS) techniques, and its photocatalytic activity was investigated in the removal of C.I. Acid Red 88 (AR88), an anionic monoazo dye of acid class, as a model contaminant. Heat treatment process at 600 °C causes an increase in crystallite size and band gap energy of TiO_2-UV100 nanoparticles. The results indicate that the nanoparticles treated for 1 h at 600 °C show the highest photocatalytic activity which can effectively degrade AR88 under UV-irradiation. Increasing heat treatment temperature above 600 °C led to reduction in TiO_2 photoactivity which may be related to the anatase-rutile phase transformation, increasing particle size and decreasing specific surface area. Removal efficiency of AR88 with heat treated TiO_2-UV100 nanoparticles was sensitive to the operational parameters such as catalyst dosage, pollutant concentration and light intensity.

1. INTRODUCTION

In recent years, it has been shown that heterogeneous photocatalysis is very promising as an alternative economical and harmless technology for the purification of wastewaters [1, 2]. Photocatalytic oxidation of organic compounds in aqueous solutions containing suspension of titanium dioxide remains a thoroughly studied method for the removal of organic and inorganic contaminants [3]. TiO_2 is an ideal photocatalyst since it is stable, inexpensive, nontoxic and highly photoactive [4, 5]. TiO_2 can be excited with UV light which promotes electrons into the conduction band and leaves

[1]Department of Chemistry, Faculty of Science, Tabriz Branch, Islamic Azad University, Tabriz, I.R. Iran; corresponding author M.A. Behnajady, e-mail: behnajady@iaut.ac.ir

holes in the valence band [6]. The high rate of electron–hole recombination on TiO_2 nanoparticles results in a low efficiency of photoactivity [7]. Various attempts have been made to reduce electron–hole recombination in photocatalytic process and to extend the absorption range of TiO_2 nanoparticles into the visible region. These include dye sensitization, coupling of another metal oxides with TiO_2, deposition of noble metal on TiO_2 crystallites and surface chelation [8, 9]. Crystal structure, particle size and surface area are considered as important factors that determine the photoactivity. For example, many studies confirmed that the anatase phase of titania is a superior photocatalytic material for air purification, water disinfection, hazardous waste remediation and water purification [8, 10, 11]. It is well known that the photocatalytic activity of TiO_2 strongly depends on the preparing methods and post-treatment conditions, since they have a decisive influence on the chemical and physical properties of TiO_2 [12, 13]. Relationship between the crystal phase, size and surface area and photocatalytic activity is very complicated. Usually heat treatment can be used to control physicochemical properties of TiO_2. How to control the heat treatment temperature and extent of phase transformation for obtaining high photocatalytic activity is still an important project [12–15]. TiO_2-UV100 nanoparticles with 8 nm crystallite size have low photocatalytic activity in comparison with other TiO_2 samples such as TiO_2-P25 nanoparticles from Degussa Co. with 21 nm crystallite size [16]. Lower photocatalytic activity in TiO_2-UV100 nanoparticles can be related to a high rate of electron-hole recombination resulting from very small crystallite size.

Presently, the effect of heat treatment on particle size, crystalline size and structure, band gap, surface area and photocatalytic activity of TiO_2-UV100 nanoparticles in the removal of C.I. Acid Red 88 (AR88) as a model contaminant from monoazo anionic dyes have been investigated. TiO_2-UV100 nanoparticles before and after heat treatment were characterized using X-ray diffraction (XRD), Brunauer –Emmett–Teller (BET) adsorption model and diffuse reflectance spectroscopy (DRS) techniques.

2. EXPERIMENTAL

Materials. AR88 monoazo anionic dye was purchased from ACROS organics (USA). The characteristics of the AR88 are summarized in Table 1. TiO_2-UV100 (Hombikat) was obtained from Sachtleben Chemie (Germany).

Characterization of heat treated TiO_2 nanoparticles. The crystallite size and phase content of TiO_2 nanoparticles were analyzed by means of the XRD measurements which were carried out at room temperature by using Siemens X-ray diffraction D5000 with CuK_α radiation (λ = 0.154056 nm). The average crystallite size (D in nm)

of TiO_2 nanoparticles was determined from XRD patterns according to the Scherrer's equation [17];

$$D = \frac{k\lambda}{\beta \cos\theta} \tag{1}$$

where k is a constant equal to 0.89, λ – the X-ray wavelength equal to 0.154056 nm, β – the full width at half maximum intensity (FWHM) and θ – the half diffraction angle. The phase content can be calculated from the integrated intensities of anatase (I_A) and rutile (I_R) peaks using the following equation [18];

$$\text{Rutile phase} = \frac{100}{1 + 0.8\left(\frac{I_A}{I_R}\right)} \quad [\%] \tag{2}$$

Table 1

Structure and characteristics of C.I. Acid Red 88 (AR88)

Structure	C.I. number	λ_{max} [nm]	M_w [g·mol^{-1}]
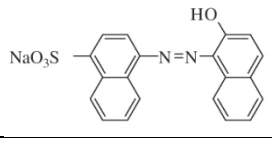	15620	506	400.39

DRS was used for determination of the optical band gap (E_g) of TiO_2-UV100 before and after heat treatment process. The following equation was used:

$$\alpha(h\nu) = B\left(h\nu - E_g\right)^{1/2} \tag{3}$$

where B is a constant dependent on the transition probability, h is Planck's constant, and ν is the frequency of the radiation. The optical absorption coefficient α was calculated from the absorbance A using the equation:

$$\alpha = 2.303\frac{A}{d} \tag{4}$$

where d is the thickness of the sample (cm) and A is the absorbance of the sample. The values of the E_g were calculated by plotting $(\alpha h\nu)^2$ vs. $h\nu$, followed by extrapolation of the linear part of the spectra to the energy axis [19]. DRS was taken using an AvaSpec-2048 TEC spectrometer.

The BET gas adsorption method has become the most widely used standard procedure for determination of the surface area of porous materials. Nitrogen (N_2) is generally the most suitable adsorptive for determination of the surface area. The standard BET procedure requires the measurement of at least three, five or more points in the appropriate pressure range on the N_2 adsorption. The BET surface area can be obtained from linear portion of BET plot. Adsorption branch was used to determine the pore size distribution using the Barret–Joyner–Halender (BJH) method [20]. BET and BJH measurements were performed using a Belsorp mini II instrument based on N_2 adsorption-desorption cycle.

Photoreactor. Photocatalytic degradation was performed in a 100 cm^3 batch quartz photoreactor with a UV lamp (15 W, UV-C, λ_{max} = 254 nm, manufactured by Philips, Holland) in a vertical array, which was placed in front of the quartz tube reactor. So, when the light intensity was measured with a Lux-UV-IR meter (Leybold Co.), the maximum intensity was observed and when the distance between the lamp and the quartz tube was increased, the light intensity decreased from 35 to 8.5 $W \cdot m^{-2}$ [21].

Procedure. A series of TiO_2-UV100 samples were treated in a muffle furnace at various temperatures (300–1000 °C) for 1 h. Another series of TiO_2-UV100 nanoparticles were heated at 600 °C at various times. All the heat-treated samples were cooled to room temperature naturally, characterized and then photocatalytic activities were tested in the removal of AR88.

In the photocatalytic degradation of AR88 a solution containing AR88 (5–35 $mg \cdot dm^{-3}$) and heat treated TiO_2 nanoparticles (300–1100 $mg \cdot dm^{-3}$) was prepared and agitated for 30 min in the darkness, then 100 cm^3 of the above suspension was transferred into the photoreactor and pure O_2 was bubbled through the reactor with the flowrate of 0.4 $cm^3 \cdot min^{-1}$. The reaction was initiated when the lamp was switched on and during irradiation, O_2 flow was maintained in the photoreactor to keep the suspension homogeneous, then at certain reaction intervals, a 5 cm^3 sample was withdrawn, centrifuged and the concentration of AR88 was determined by means of a UV-vis spectrophotometer (Ultrospec 2000, England) at 506 nm.

3. RESULTS AND DISCUSSION

3.1. THE CHARACTERIZATION OF TIO_2-UV100 NANOPARTICLES

TiO_2 materials exist in three different crystalline forms: anatase, rutile and brookite. The XRD patterns of TiO_2-UV100 and heat treated TiO_2-UV100 at two temperatures (600 and 900 °C) and various heat treatment times are shown in Fig. 1, for 2θ diffraction angles between 4° and 70°.

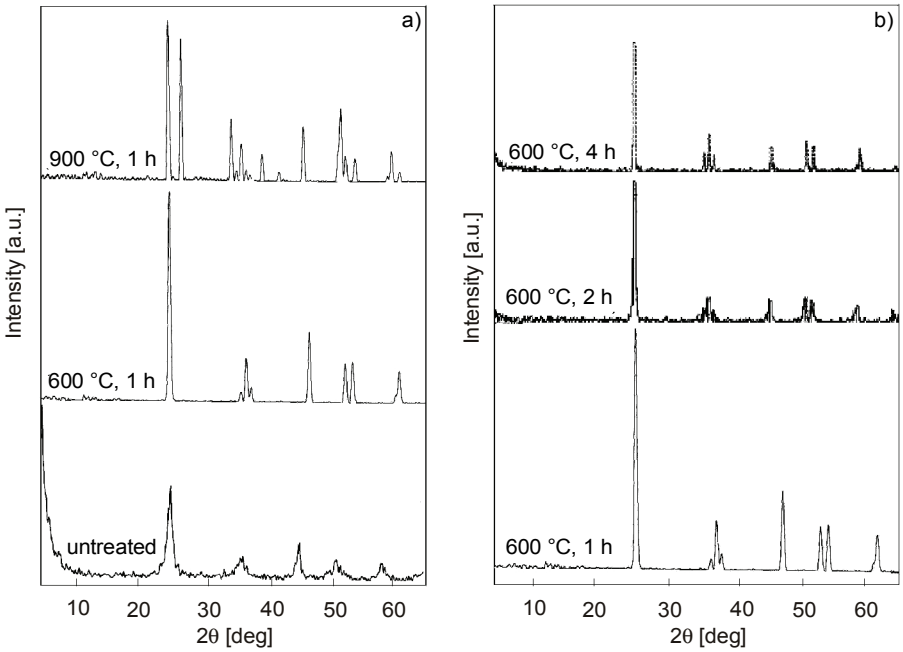

Fig. 1. XRD patterns of heat treated TiO_2-UV100 powders at various temperatures (a) and after various times (b)

These results indicate that TiO_2-UV100 is 100% anatase, and no rutile phase was detected in heat treated TiO_2 at 600 °C. The XRD patterns of heat treated TiO_2-UV100 at various temperatures in Fig. 1a show that phase transformation takes place at 900 °C. Wang et al. [13] reported for 100 nm TiO_2, phase transformation from anatase to rutile which takes place at 400 °C. Also results reported by Yu et al. [10] indicated that the molar ratios of $EtOH/H_2O$ greatly influenced the crystallinity, crystallite size and temperature of phase transformation from anatase to rutile which was reported to occur at 700 °C. It seems that the crystallite size and granularity of TiO_2 are the most important factors determining the temperature of phase transformation [12, 13, 22].

The average crystallite size for TiO_2-UV100, and heat-treated TiO_2-UV100 at 600 and 900 °C were obtained from maximum intensity of anatase phase at 25.2° as 8, 19 and 28 nm, respectively. All samples were 100% anatase but heat treated sample at 900 °C was 48% anatase and 52% rutile. The XRD patterns of heat treated TiO_2--UV100 at 600 °C after 1, 2 and 4 h heat treatment showed that all samples were 100% anatase but increasing heat treatment time causes an increase in crystallite size as 19, 35 and 42 nm, respectively (Fig. 1b).

Absorption spectra of TiO_2-UV100 nanoparticles and heat treated sample at 600 °C are shown in Fig. 2. E_g values can be calculated from Fig. 3 by extrapolation of the linear part of the spectra to the energy axis. Results indicate that heat treatment of

TiO_2-UV100 at 600 °C increased the optical band gap energy from 3.13 to 3.25 eV. The different band gap energies might be attributed to the difference in the surface microstructure, composition and phase structure in the TiO_2 nanoparticles [12].

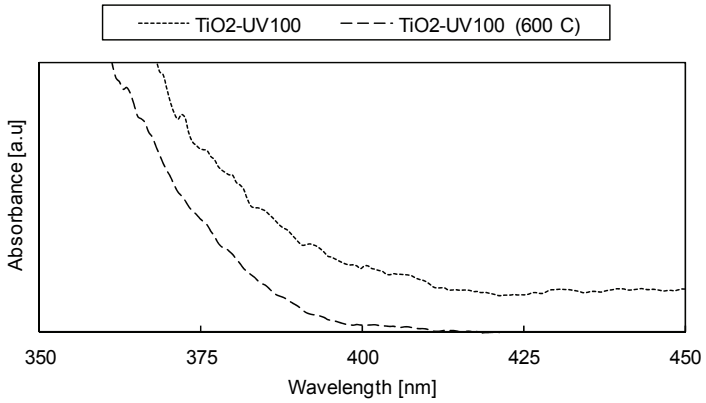

Fig. 2. Diffuse reflectance spectra of untreated and heat treated for 1 h TiO_2-UV100

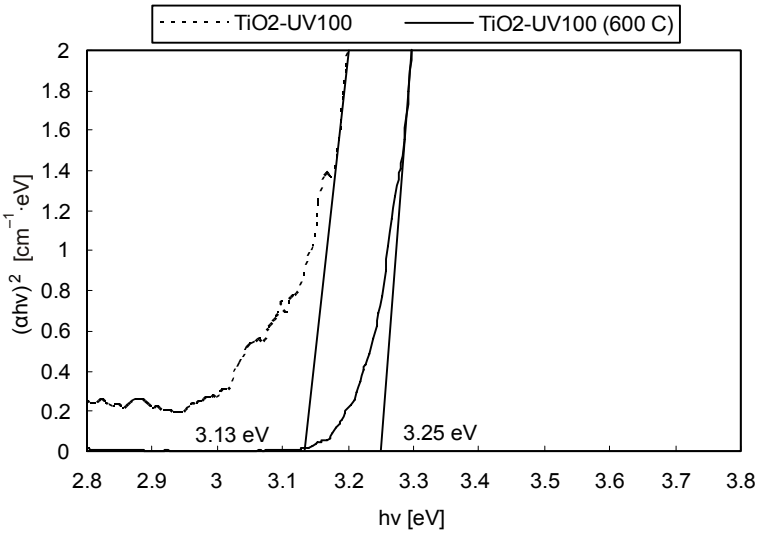

Fig. 3. Plot of $(\alpha h\nu)^2$ vs. $h\nu$ for untreated and heat treated for 1 h TiO_2-UV100

Heat treatment of TiO_2-UV100 nanoparticles leads to changes in BET surface area, pore volume and pore size distribution. Figures 4 and 5 show the nitrogen adsorption-desorption isotherms and pore size distribution curves calculated by the Barrett–Joyner–Helenda (BJH) method for heat treated TiO_2-UV100 at 600 and 900 °C, respectively. The BET surface area obtained from the linear portion of BET plot and pore size information of the samples determined by the BJH method have been sum-

marized in Table 2 [20]. According to the results in Table 2, the heat treated sample at 600 °C has 19.15 $m^2 \cdot g^{-1}$ surface area.

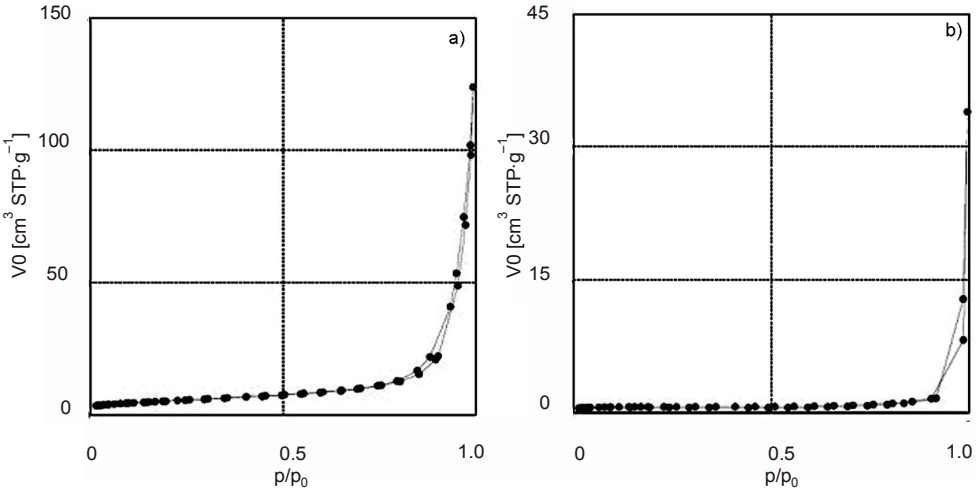

Fig. 4. Nitrogen adsorption and desorption isotherms of heat treated for 1 h TiO_2-UV100 at 600 °C (a) and 900 °C (b). V_a is the volume adsorbed and p/p_0 is the relative pressure

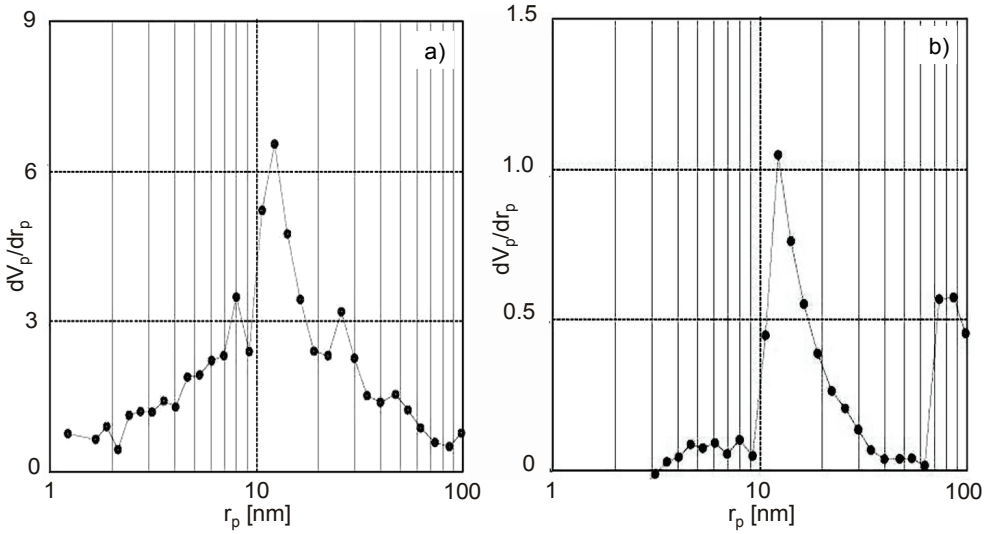

Fig. 5. Pore size distribution curves calculated from the adsorption branch of heat treated for 1 h TiO_2-UV100 at 600 °C (a) and 900 °C (b). V_p is the pore volume and r_p is pore size

This value is much lower than that for untreated TiO_2-UV100 (350 $m^2 \cdot g^{-1}$). This is due to the increase in average crystallite size and pore collapse of the heat treated TiO_2

powders [3, 23]. In the result of sintering and phase transformation of anatase to rutile, the BET surface area decreased drastically to 2.58 $m^2 \cdot g^{-1}$ for TiO_2-UV100 heat treated at 900 °C. Pore size distribution measurement indicates upon increasing heat treatment temperature, the pore structure of TiO_2-UV100 nanoparticles changes from micropores to mesopores. The mesopore structure of heat treated TiO_2-UV100 nanoparticles is attributed to pores formed between TiO_2 particles [10]. In addition, the larger pores may be due to the formation of inter-agglomeration particles [23, 24]. The results show that pore volume decreases significantly with increasing heat treatment temperature. This decrease is attributed mainly to partial pore collapse or shrinkage after heat treatment at higher temperatures [23].

Table 2

The BET surface area and pore parameters of untreated and heat treated for 1 h TiO_2-UV100

Photocatalyst	BET surface area [$m^2 \cdot g^{-1}$]	Most distribution pore size [nm]	Mean pore diameter [nm]	Total pore volume [$cm^3 \cdot g^{-1}$]
TiO_2-UV100	350.81	1.21	5.99	0.5255
TiO_2-UV100 (600 °C, 1 h)	19.15	12.24	33.52	0.1605
TiO_2-UV100 (900 °C, 1 h)	2.58	12.24	46.097	0.0298

3.2. PHOTOCATALYTIC ACTIVITY

The catalyst activity was evaluated using the photodegradation of AR88 as a model pollutant under UV irradiation. The degradation efficiency of organic pollutant is a function of photocatalyst parameters, such as the crystalline phase, particle size, band gap and surface area. All TiO_2-UV100 samples have photocatalytic activity in the removal of AR88.

Figure 6 shows semi-logarithmic plots of the concentration of AR88 in the presence of various heat treated TiO_2-UV100 nanoparticles vs. irradiation time. The highest level of degradation was obtained with TiO_2 treated for 1 h at 600 °C. Figure 7 shows that the apparent first-order reaction rate constant (k_{ap}) (obtained from the slopes of the lines in Fig. 6) increased with increasing heat treatment temperature until 600 °C and then decreased. XRD results indicate that with increasing heat treatment temperature to 600 °C, only pure anatase TiO_2 phase exists, therefore the enhanced activity of heat treated TiO_2 cannot be attributed to phase transformation. But according to XRD results, average crystallite size for heat treated TiO_2-UV100 at 600 °C increases to 19 nm. There is an optimum particle size in the nanocrystalline TiO_2 system for maximum photocatalytic activity. At optimum particle size in nanocrystalline TiO_2 recombination of e^- and h^+ is less effective than interfacial charge-carrier transfer processes [16, 25]. A large surface area may be an important factor, influencing the

rate of photocatalytic degradation process, as a large amount of adsorbed organic molecules promote the photocatalytic reaction [26].

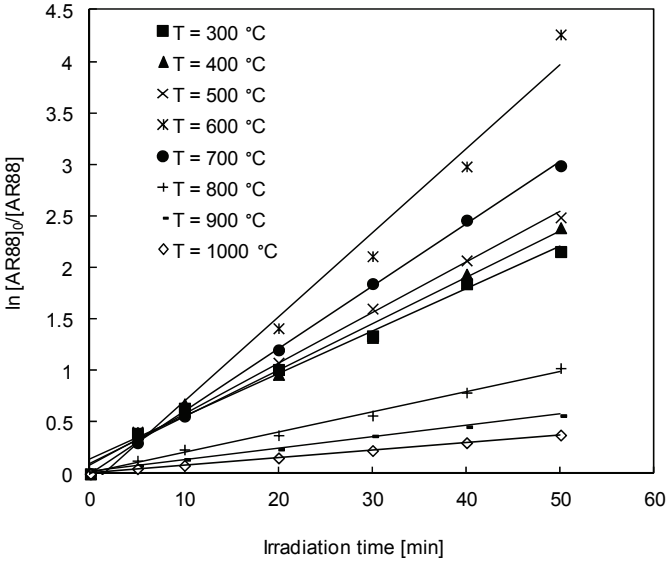

Fig. 6. Semi-logarithmic plots of the concentration of AR88 at various heat treatment temperatures of TiO_2-UV100 vs. irradiation time. [TiO_2-UV100] = 300 mg·dm^{-3}, [AR88]$_0$ = 20 mg·dm^{-3}, I_0 = 37 W·m^{-2}

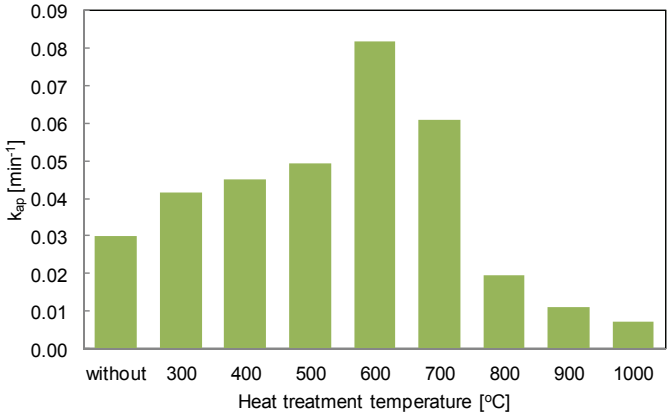

Fig. 7. Apparent first-order reaction rate constant vs. heat treatment temperature of TiO_2-UV100. [TiO_2-UV100] = 300 mg·dm^{-3}, [AR88]$_0$ = 20 mg·dm^{-3}, I_0 = 37 W·m^{-2}

Results of this work indicate that in comparison with other parameters, the surface area is not a significant parameter in photocatalytic activity; heat treated TiO_2-UV100 at 600 °C with highest photocatalytic activity has very low surface area in comparison

with untreated TiO_2-UV100 (350 $m^2 \cdot g^{-1}$). Also, TiO_2-UV100 with a large surface area may be is associated with large amounts of crystalline defects which favour recombination of photogenerated electrons and holes, leading to a poor photocatalytic activity in comparison with heat treated TiO_2-UV100 at 600 °C [3, 27]. On the other hand, due to the higher band gap energy of heat treated TiO_2-UV100 at 600 °C compared to that of untreated one, the heat treated samples are expected to have a higher photoactivity in photooxidation and photoreduction than untreated TiO_2-UV100. Lower photocatalytic activity of heat treated TiO_2-UV100 at 900 °C can be attributed to phase transformation from anatase to rutile phase. TiO_2 in rutile form is less effective than in the anatase form as a photocatalyst for the oxidation of most organic compounds [14]. Therefore, it is expected that heat treated TiO_2 at 1000 °C has lower photoactivity than heat treated TiO_2 at other temperatures.

3.3. EFFECT OF OPERATIONAL PARAMETERS ON PHOTOCATALYTIC ACTIVITY OF HEAT TREATED TiO_2-UV100 AT 600 °C

Figure 8 shows the effect of various dosages of heat treated TiO_2-UV100 at 600 °C on the photocatalytic removal of AR88.

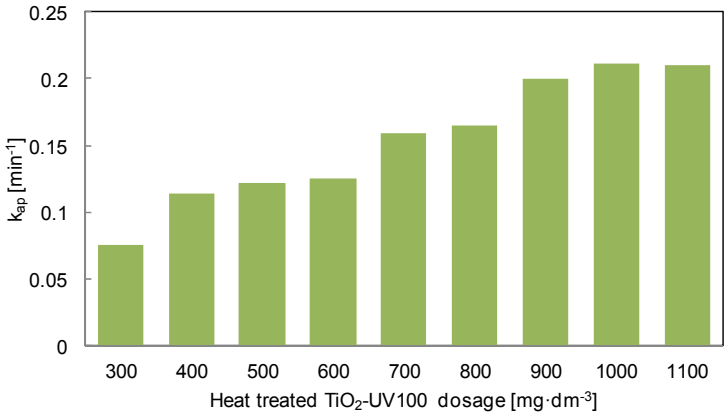

Fig. 8. Apparent first-order reaction rate constant vs. various dosages of heat treated TiO_2-UV100 (600 °C, 1 h). $I_0 = 35$ W·m^{-2}, $[AR88]_0 = 20$ mg·dm^{-3}

The k_{ap} was found to increase with increasing the amount of TiO_2 until 1000 mg·dm^{-3} so that removal reaches to 96% under 15 min of irradiation time. The observed enhancement in this range is probably due to an increased number of available adsorption and catalytic sites on TiO_2. Improvement on the removal rate is not obvious above 1000 mg·dm^{-3}, because at high catalyst loading, turbidity of solution and scattering effect increase which cause a decrease in UV light penetration to the solution [1, 16, 28, 29]. Figure 9 shows the effect of heat treatment time on the k_{ap} in presence

of 1000 mg·dm^{-3} heat treated TiO_2 at 600 °C. Results show that the highest level of photoactivity was obtained with 1 h heat-treated TiO_2. Decreasing photocatalytic activity with increasing heat treatment time above 1 h can be related to the increase of crystallite size according to the XRD results.

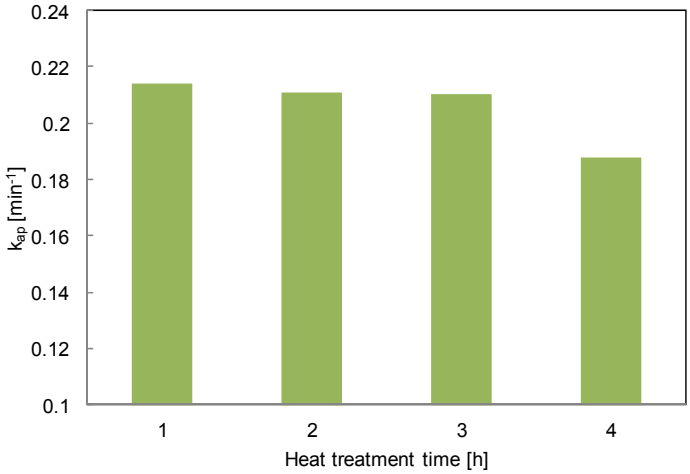

Fig. 9. Apparent first-order reaction rate constant vs. heat treatment time of TiO_2-UV100. [Heat treated TiO_2-UV100 (600 °C, 1 h)] = 1000 mg·dm^{-3}, $[AR88]_0$ = 20 mg·dm^{-3}, I_0 = 35 W·m^{-2}

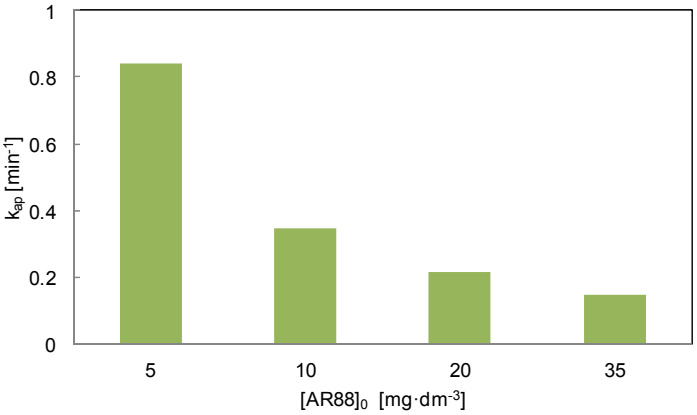

Fig. 10. Apparent first-order reaction rate constant vs. initial concentration of AR88. I_0 = 35 W·m^{-2}, [Heat treated TiO_2-UV100 (600 °C, 1 h)] = 1000 mg·dm^{-3}

The influence of the initial concentration of AR88 on the removal of AR88 has been investigated using various initial concentrations of AR88 varying from 5 to 35 mg·dm^{-3}. The results illustrated in Fig. 10 indicate that the k_{ap} decreases with increasing AR88 initial concentration and removal percent decreases from 99 to 60% un-

der 5 min of irradiation time. This result is reasonable because with increasing initial concentration of AR88 decreases the light intensity that falls onto the surface of TiO_2. On the other hand, with increasing AR88 initial concentration more and more organic substances are adsorbed on the surface of TiO_2 and consequently the generation of hydroxyl radicals on the surface of TiO_2 and also degradation efficiency decreases [13, 16].

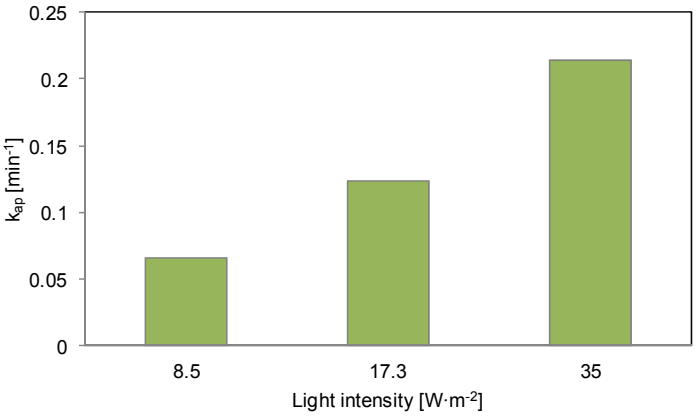

Fig. 11. Apparent first-order reaction rate constant vs. light intensity.
$[AR88]_0$ = 20 mg·dm^{-3}, [Heat treated TiO_2-UV100 (600 °C, 1 h)] = 1000 mg·dm^{-3}

The dependences of k_{ap} on UV light intensity in the removal of AR88 with heat treated TiO_2-UV100 under optimum conditions are shown in Fig. 11. It is evident that k_{ap} increases with the increasing light intensity from 8.5 to 35 W·m^{-2}, so that the removal increases from 62% to 96% under 15 min of irradiation time. The UV irradiation generates photons required for the electron transfer from the valence band to the conduction band of a semiconductor photocatalyst. The rate of degradation increases when more radiation falls on the catalyst surface and hence more hydroxyl radicals are produced [16, 30].

4. CONCLUSIONS

The results of this work indicate that the heat treatment temperature strongly influences the structure and photocatalytic activity of TiO_2. An optimum particle size was found in nanocrystalline TiO_2 system for maximum photocatalytic activity. Heat-treated TiO_2-UV100 at 600 °C within 1 h with 19 nm crystallite size has the highest photocatalytic activity in comparison with other heat-treated samples. Increasing the band gap of heat-treated TiO_2-UV100 at 600 °C is another reason for higher photocatalytic activity. Phase transformation for TiO_2-UV100 nanoparticles takes place at 900 °C which causes a decrease in the photocatalytic activity. Photoactivity of heat-

treated TiO_2-UV100 under optimum conditions increases with increasing TiO_2 slurry dosage, UV-light intensity and decreasing the initial AR88 concentration.

ACKNOWLEDGEMENTS

The authors would like to thank the Tabriz branch, Islamic Azad University for financial support and the Iranian Nanotechnology Initiative Council.

REFERENCES

[1] DANESHVAR N., RABBANI M., MODIRSHAHLA N., BEHNAJADY M.A., *Kinetic modeling of photocatalytic degradation of Acid Red 27 in UV/TiO_2 process*, J. Photochem. Photobiol. A, 2004, 168 (1–2), 39.

[2] BEHNAJADY M.A., MODIRSHAHLA N., HAMZAVI R., *Kinetic study on photocatalytic degradation of C.I. Acid Yellow 23 by ZnO photocatalyst*, J. Hazard. Mater., 2006, 133 (1–3), 226.

[3] BAKARDJIEVA S., SUBRT J., STENGL V., DIANEZ M.J., SAYAGUES M.J., *Photoactivity of anatase-rutile TiO_2 nanocrystalline mixtures obtained by heat treatment of homogeneously precipitated anatase*, Appl. Catal. B, 2005, 58 (3–4), 193.

[4] HOFFMANN M.R., MARTIN S.T., CHOI W., BAHNEMNN D.W., *Environmental applications of semiconductor photocatalysis*, Chem. Rev., 1995, 95 (1), 69.

[5] SEERY M.K., GEORGE R., FLORIS P., PILLAI S.C., *Silver doped titanium dioxide nanomaterials for enhanced visible light photocatalysis*, J. Photochem. Photobiol. A, 2007, 189 (2–3), 258.

[6] FUJISHIMA A., RAO T.N., TRYK D.A., *Titanium dioxide photocatalysis*, J. Photochem. Photobiol. C, 2000, 1 (1), 1.

[7] SOBANA N., MURUGANADHAM M., SWAMINATHAN M., *Nano-Ag particles doped TiO_2 for efficient photodegradation of Direct azo dyes*, J. Mol. Catal. A, 2006, 258 (1–2), 124.

[8] VAMATHEVAN V., AMAL R., BEYDOUN D., LOW G., MCEVOY S., *Photocatalytic oxidation of organics in water using pure and silver-modified titanium dioxide particles*, J. Photochem. Photobiol. A, 2002, 148 (1–3), 233.

[9] RAO K.V.S., LAVÉDRINE B., BOULE P., *Influence of metallic species on TiO_2 for the photocatalytic degradation of dyes and dye intermediates*, J. Photochem. Photobiol. A, 2003, 154 (2–3), 189.

[10] YU J.C., YU J., ZHANG L., HO W., *Enhancing effects of water content and ultrasonic irradiation on the photocatalytic activity of nanosized TiO_2 powders*, J. Photochem. Photobiol. A, 2002, 148 (1–3), 263.

[11] KAWAHARA T., OZAWA T., IWASAKI M., TADA H., ITO S., *Photocatalytic activity of rutile- anatase coupled TiO_2 particles prepared by a dissolution-reprecipitation method*, J. Colloid Interface Sci., 2003, 267 (2), 377.

[12] YU J., YU H., CHENG B., ZHOU M., ZHAO X., *Enhanced photocatalytic activity of TiO_2 powder (P25) by hydrothermal treatment*, J. Mol. Catal. A, 2006, 253 (1–2), 112.

[13] WANG J., ZHAO G., ZHANG Z., ZHANG X., ZHANG G., MA T., JIANG Y., ZHANG P., LI Y., *Investigation on degradation of azo fuchsine using visible light in the presence of heat-treated anatase TiO_2 powder*, Dyes Pigm., 2007, 75 (2), 335.

[14] MACHADO N.R.C.F., SANTANA V.S., *Influence of thermal treatment on the structure and photocatalytic activity of TiO_2 P25*, Catal. Today, 2005, 107–108 (2), 595.

[15] TAKAHASHI J., ITOH H., MOTAI, S.SHIMADA S., *Dye adsorption behavior of anatase- and rutile-type TiO_2 nanoparticles modified by various heat-treatments*, J. Mater. Sci., 2003, 38 (8), 1695.

[16] BEHNAJADY M.A., MODIRSHAHLA N., SHOKRI M., ELHAM H., ZEININEZHAD A., *The effect of particle size and crystal structure of titanium dioxide nanoparticles on the photocatalytic properties*, J. Environ. Sci. Health A, 2008, 43 (5), 460.
[17] PATTERSON A.L., *The Scherrer formula for X-ray particle size determination*, Phys. Rev., 1939, 56 (10), 978.
[18] SPURR R.A., MYERS H., *Quantitative analysis of anatase-rutile mixtures with an X-ray diffractometer*, Anal. Chem., 1957, 29 (5), 760.
[19] ABDUL-KADER A.M., *Modification of the optical band gap of polyethylene by irradiation with electrons and gamma rays*, Philos. Mag. Lett., 2009, 89 (3), 162.
[20] SING K.S.W., EVERETT D.H., HAUL R.A.W., MOSCOU L., PIEROTTI R.A., ROUQUEROL J., SIEMIENIEWSKA T., *Reporting physisorption data for gas/solid systems with special reference to the determination of surface area and porosity*, Pure Appl. Chem., 1985, 57 (4), 603.
[21] BEHNAJADY M.A., ESKANDARLOO H., MODIRSHAHLA N., SHOKRI M., *Investigation of the effect of sol–gel synthesis variables on structural and photocatalytic properties of TiO_2 nanoparticles*, Desalination, 2011, 278 (1–3), 10.
[22] KIM C.S., KWON I.M., MOON B.K., JEONG J.H., CHOI B.C., KIM J.H., CHOI H., YI S.S., YOO D.H., HONG K.S., PARK J.H., LEE H.S., *Synthesis and particle size effect on the phase transformation of nanocrystalline TiO_2*, Mater. Sci. Eng. C, 2007, 27 (5–8), 1343.
[23] CHEN Y., DIONYSIOU D.D., *Correlation of structure properties and film thickness to photocatalytic activity of thick TiO_2 films coated on stainless steel*, Appl. Catal. B, 2006, 69 (1–2), 24.
[24] PORTER J.F., LI Y.G., CHAN C.K., *The effect of calcination on the microstructural characteristics and photoreactivity of Degussa P-25 TiO_2*, J. Mater. Sci., 1999, 34 (7), 1523.
[25] BEYDOUN D., AMAL R., LOW G., MCEVOY S., *Role of nanoparticles in photocatalysis*, J. Nanopart. Res., 1999, 1 (4), 439.
[26] KRYSA J., KEPPERT M., JIRKOVSKY J., STENGL V., SUBRT J., *The effect of thermal treatment on the properties of TiO_2 photocatalyst*, Mater. Chem. Phys., 2004, 86 (2–3), 333.
[27] LV K., XIANG Q., YU J., *Effect of calcination temperature on morphology and photocatalytic activity of anatase TiO_2 nanosheets with exposed {001} facets*, Appl. Catal. B, 2011, 104 (3–4), 275.
[28] KONSTANTINOU I.K., ALBANIS T.A., *TiO_2-assisted photocatalytic degradation of azo dyes in aqueous solution: kinetic and mechanistic investigation*, Appl. Catal. B, 2004, 49 (1), 1.
[29] GONÇALVES M.S.T., PINTO E.M.S., NKEONYE P., OLIVEIRA-CAMPOS A.M.F., *Degradation of C.I. Reactive Orange 4 and its simulated dyebath wastewater by heterogeneous photocatalysis*, Dyes Pigm., 2005, 64 (2), 135.
[30] BEHNAJADY M.A., MODIRSHAHLA N., DANESHVAR N., RABBANI M., *Photocatalytic degradation of an azo dye in a tubular continuous-flow photoreactor with immobilized TiO_2 on glass plates*, Chem. Eng. J., 2007, 127 (1–3), 167.